Benefit Assessment of Commercial Synthetic Aperture Radar Observations for NASA's Surface Deformation and Change Mission Study

B. Osmanoglu[1*], S. A. Huang[1], C. A. Jones[2], B. Scheuchl[3], A. Khazendar[4], J. Sauber[1], K. Tymofyeyeva[4], M.J. Jo[1]

[1] NASA Goddard Space Flight Center, Greenbelt, MD, U.S.A. - (batuhan.osmanoglu, stacey.a.huang, jeanne.m.sauber-rosenberg, minjeong.jo)@nasa.gov

[2] Langley Research Center, Hampton, VA, U.S.A. - christopher.a.jones-2@nasa.gov

[3] University of California, Irvine, CA, U.S.A. - bscheuch@uci.edu

[4] Jet Propulsion Laboratory, California Institute of Technology, Pasadena, CA, U.S.A. – (ala.khazendar, katia.tymofyeyeva)@jpl.nasa.gov

KEY WORDS: Synthetic Aperture Radar, Commercial SAR, Surface Deformation and Change.

ABSTRACT:

The Surface Deformation and Change (SDC) mission study is investigating a synthetic aperture radar (SAR) mission that is expected to launch in the next decade, building on the foundation established by the NASA ISRO Synthetic Aperture Radar (NISAR) mission. Since 2019, the SDC study team has updated the observation needs identified by the 2017 Earth Science Decadal Survey, developing a Science and Applications Traceability Matrix (SATM) that includes an expanded set of geophysical observables (GOs). These needs were further refined by a team of discipline experts, resulting in 48 GOs. For each GO, imaging characteristics such as revisit, accuracy, resolution, polarisation, data latency, are defined in the SATM. This paper describes the benefit assessment methodology, provides an example to generate current commercial feasibility scores for each GO in the SATM, even though the SDC mission will not be launched until the next decade. This methodology generates a quantitative assessment of commercial SAR data in meeting the measurement needs of a GO defined in SDC's SATM. Our assessment suggests that current commercial SAR data are particularly useful for constraining geophysical processes that benefit from short-repeat acquisition times and high spatial resolution.

1. INTRODUCTION

Guided by the SATM (Horst et al. 2021, Khazendar et al. 2021), the SDC mission study is evaluating several architectures having different numbers of spacecraft, orbital configurations, sensor characteristics, and geometries. These configuration differences result in distinct core capabilities, which are evaluated in a consistent value framework.

Some of these core capabilities can benefit from commercial SAR constellations filling in data gaps, especially in terms of high temporal and spatial resolutions. In recent years, commercial sector capabilities in SAR imaging have been expanding rapidly, however, the interferometric capability is currently still limited. The feasibility of commercial capabilities to support the GOs defined in SDC's SATM are being analysed to identify the strengths and weaknesses of commercial SAR data when applied to SDC observables. In addition to the parameters defined in the SATM, our analysis also looks at the interferometric capability of commercial constellations, along with their swath width and their global sampling coverage rate. The GOs are described in detail in the SATM, and a summary of the relevant parameters used in the scoring is provided in the appendix. To achieve a result that is resilient in the face of market fluctuations, the commercial assessment relies on studying industry capabilities as a whole instead of individually focusing on each constellation.

2. METHODOLOGY

The methodology is designed to assess possible strengths and weaknesses of commercial SAR data in meeting the GOs defined in SDC's SATM. The scoring equation uses eight key factors to parameterize the benefit of commercial data for each GO.

2.1 Parameters

All parameters defined in this assessment are defined as a percentage, represented as a number between 0 and 1 for low and high scores, respectively. Table 1 lists these parameters, how they affect the score in (1), their description, and the equation to calculate each factor.

Parameter	Type	Description	Eq.
Polarisation	Additive	Percent channels available vs. desired in SATM	$min(1, \frac{cc}{satm})$
Resolution	Additive	Inverse percentage of available resolution vs. SATM.	$min(1, \frac{satm}{cc})$
Revisit	Additive	Inverse percentage of available revisit vs. SATM.	$min(1, \frac{satm}{cc})$
Latency	Additive	Inverse percentage of available revisit vs. SATM.	$min(1, \frac{satm}{cc})$
Coverage	Multiplicative	Percentage of available vs. requirement	$min(1, \frac{cc}{req.})$
Large Swath	Multiplicative	Percentage of large swath capable constellations	No = 1.0 Yes & No = $\frac{1+perc}{2}$ Yes = $perc$
InSAR	Multiplicative	Percentage of SAR capable constellations.	No = 1.0 Yes & No = $\frac{1+perc}{2}$ Yes = $perc$
*Accuracy	Minimum	Accuracy percentage for the given geophysical observable either through heuristic or literature survey.	$min(1, \frac{satm}{lit.svy})$

Table 1. Parameters used in the scores.
*The equation is only used for literature survey results when heuristic scores are not available.

Benefit scores are calculated using the following equations:

$$score_{int} = \frac{1}{N}\sum_{i}^{N} S_i \times \prod_{j}^{M} C_j \quad (1)$$

$$score_{fin} = min(acc, score_{int}) \quad (2)$$

where $score_{int}$ is the interim score, N is the number of parameters that are arithmetically averaged, and M is the number of multiplicative parameters (defined in Table 1). S and C represent the partial scores, $score_{fin}$ is the final score, and acc is expected measurement accuracy (relative to the desired capability in the SATM, see example in Table 4).

In (1), arithmetic averaging is used in the partial scores S and multiplication is used in the partial scores C due to the perceived difference in the impact of these parameters. For example, if data can be acquired every two weeks, but the desire is to collect data every week, the revisit score would be 50%. We equally weighted revisit, polarisation, resolution, and latency, therefore arithmetic averaging is used for a combined S score. On the other hand, coverage, large swath imaging, and InSAR capabilities are more limiting compared to parameters contributing to the S score. For example, if global coverage is needed every two weeks, and there is only enough commercial capacity to image 50% of the globe every two weeks, this should not result in a C score that is higher than the lowest factor, even if InSAR and large-swath capacity are fully met. Therefore the C scores are multiplicative as shown in (2).

As part of the commercial SAR feasibility assessments, the team identified the main observational parameters and associated representative capabilities that commercial SAR can currently provide, as shown in Table 2.

Parameter	Value	Justification
Polarisation	Single	Commercial market capability currently focuses on co-pol observations
Resolution	5m	Commercial imagery is capable of delivering higher resolution at the expense of measurement noise level.
Revisit	1 day	Commercial constellations are aiming to deliver data at a daily frequency anywhere in the world. At the moment this is aspirational for interferometry and demonstrated for radiometry.
Latency	4 hours	Most commercial vendors provide low latency downlink
Coverage	2.21M km^2/ day	At the time of the assessment, the commercial market had a combined capacity of over 2.21M km^2 per day.
Large Swath	0.43	Four out of the seven active constellations support collecting >100 km wide imagery for large area coverage
InSAR	0.43	Four out of the seven active constellations support collecting interferometric data at least in part of their constellation.
Accuracy	Variable	The value ranges from 0% to 100% based on the expected performance.

Table 2. An overview of currently available representative commercial capabilities used in the commercial SAR feasibility estimation

These capabilities are derived from publicly available information from the commercial constellations operated by Capella Space, ICEYE, iQPS, NEC, Surrey Sat. Tech. Ltd, Synspective, and Umbra. One important parameter that is not considered in the above set of parameters is the satellite frequency band. This is due to the fact that the bulk of the available commercial data is in X-band. Rather than excluding GOs that desire a specific band, we estimate expected performance at X-band for all GOs with the assumption that any GO can be satisfied under specific observation scenarios or locations, even if they cannot be satisfied globally at X-band. However, depending on the target of interest, X-band sensors can fall short for Ecosystems and Solid Earth observables due to shallow penetration depth and rapid decorrelation (Zebker and Villasenor, 1992; Wei and Sandwell, 2010; Hajj et al., 2019). In some cases, imaging might still be possible, albeit with significantly less coverage and accuracy compared to a longer wavelength sensor; in other cases, however, the sensors may completely fail to retrieve any meaningful measurements. In particular, long-wavelength radar can be critical for observing change mapping in wetlands, forests, and coastal zones (Ottinger and Kuenzer, 2020), and for imaging subtle movements of faults in heavily vegetated areas (Nikolaeva et al., 2014; Tong et al., 2018). Here, we have not explicitly accounted for the cases in which X-band sensors would completely fail to return meaningful data, but these limitations are important to consider in the overall evaluation of commercial SAR capabilities. For the GOs that are not assessed by the performance tool, a literature review was conducted to approximate the measurement capability at X-band, and for heuristic scores the expert panel provided accuracy estimates considering X-band. Ultimately, a percentage of desired capability is calculated based on this value and the SATM is used in the assessment (see Table 4).

Coverage may require special attention in this calculation as this capability is defined by km^2/day for the average commercial market, while the SATM did not define such a metric, assuming a global need. Unlike the value framework assessment for SDC architectures, a coverage area is defined in the commercial assessment for each geophysical observable, as shown in Table 3.

Global	129 M km^2	Total land area
Continental	25 M km^2	
Regional	9 M km^2	About the size of the US or EU
Local	1 M km^2	

Table 3. Coverage bins used in this study for each GO.

Table 3 is used to check the capability of the commercial sector to see if such an area can be covered during the required revisit time defined for the GO.

Even though the same SATM is used for both the value framework analysis and the commercial SAR assessment, the assessments are different to compensate for the differences between commercial capabilities and SDC architectures. For example, all SDC architectures provide coverage of all land and ice areas every 12 days or faster, and it is not feasible to acquire global coverage using commercial constellations due to coverage limitations and cost. Similarly, all SDC architectures are capable of interferometry, while only three out of seven commercial constellations provide that capability. Such differences necessitate the use of additional parameters for the commercial SAR assessment.

2.2 Scoring

The assessment scores each GO against the needs defined in the SATM. For example, the ninth ecosystem (E9) GO calls for "measuring inland coastal wetland areas" and mentions the need for dual polarisation imagery at 20 m resolution with a revisit and latency of 14 days (Table 4). Similarly, the need for coverage is classified as regional (9 million km^2) every 14 days, and neither large swath imagery nor interferometry are necessary (Table 5). Our panel of experts assessed the X-band performance of wetland mapping as 35%.

Parameter	Polar. (#)	Resol. (m)	Revisit (day)	Latency (day)	Arithmetic Average
Need	2	20	14	14	
Capability	1	5	1	0.16	
Part. Score	0.5	1	1	1	0.875

Table 4. Example estimation of percent capabilities addressing the desired needs for parameters defined in the SATM (GO E9).

Parameter	Coverage (km^2/day)	Large Area Imaging	InSAR	Multiplication Result
Need	Regional @14 days (revisit)	No	No	
Capability	2.2e6	0.43	0.43	
Part. Score	1	1	1	1.0

Table 5. Example estimation of percent capabilities addressing the desired needs for Commercial SAR assessment specific parameters (GO E9).

$$score_{int} = 0.875 \times 1.0 = 0.875 \quad (3)$$

$$score_{fin} = min(0.35, 0.875) = 0.35 \quad (4)$$

Where $score_{int}$ is calculated based on the multiplication of partial scores in Table 4 and Table 5. By design of (2) the final score is limited with the accuracy parameter.

3. RESULTS

This methodology was applied to all of the GOs in the SATM to produce a self-consistent set of commercial benefit scores. These results allow for identification of GOs that would benefit more than others in a relative sense.

3.1 Comparative Assessment

In order to better understand the benefit of commercial data, an architecture based on a simplified NISAR design (Kellog et al. 2020, Rosen et al. 2021), which we call as L1A, was assessed. The relevant parameters of this design are summarised in Table 6.

Parameter	Pol. (#)	Res. (m)	Rev. (day)	Lat. (day)	Cov. (km^2/d)	Large Area	InSAR
Capability	4	5	12	1	10.8e6	1.0	1.0

Table 6. Conservative capability estimate of L1A architecture for this analysis.

The accuracy scores for L1A came from a Value Framework in development for assessing the SDC architectures with respect to Science Benefit and other components of Value. In the Value Framework, accuracy metrics for each GO can depend on either or both vertical and horizontal accuracy needs. In cases where more than a single accuracy score was provided, these scores were averaged to obtain GO specific L1A accuracy score. These scores then compare the capability of an architecture to the desired capability in the SATM for each GO, and quantify the degree to which that architecture achieves the SATM's needs.

Figures 1 and 2 show the relationship between the commercial constellations vs. L1A scores, separating the GOs based on the source of the accuracy metric, heuristic, and performance tool, respectively. There are two reasons for this: 1) the performance tool accuracy calculation is holistic and accounts for parameters such as revisit rates as well; and 2) due to the very different nature of accuracy estimates and the strong control of accuracy on the final outcome, the behaviour of GOs for both cases needs to be investigated.

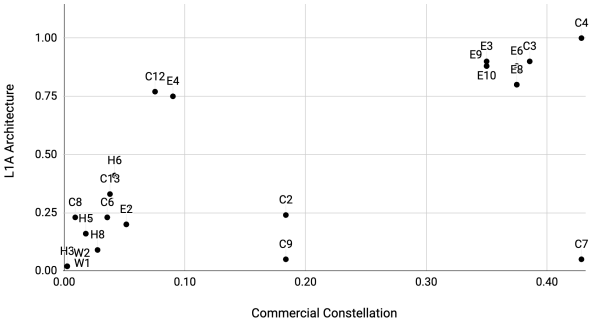

Figure 1. Commercial assessment scores against L1A architecture for GOs with heuristic accuracy.

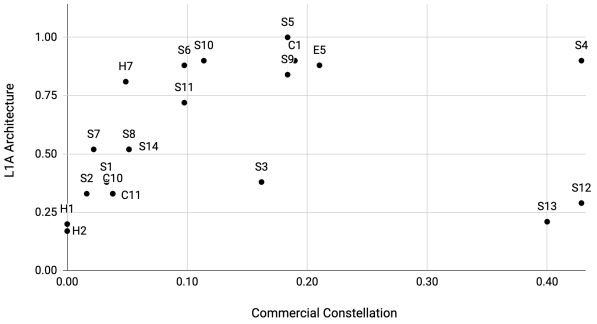

Figure 2. Commercial assessment scores against L1A architecture for GOs with performance tool based accuracy.

Figures 1 and 2 demonstrate a logarithmic nature, with a sharp rise close to the origin and relative flattening at the far end of the x-axis. This behaviour is perhaps indicative of the fact that both SAR systems are capable of addressing the SATM albeit less so for commercial constellations. Furthermore, the different range of scores are evident, as commercial assessment scores achieve a high of only 0.43 while the L1A architecture does achieve a full score (1.0) for some GOs. On average, L1A scores an average of 0.49, while commercial constellations achieve a score of 0.15 in realising the SDC SATM. Despite this, there are some GOs that achieve higher assessment scores for the commercial constellation compared to L1A, such as cryospheric GOs C7 and C9, as well as solid Earth GOs such as S12, S13.

4. DISCUSSION

The effort documented here covers only an augmentation of a core SDC capability. The SDC team has also reached out to the industry through a Request For Information (RFI) and is planning to release a Request for Proposal (RFP) in the first quarter of 2023. The RFI/RFP activities include public-private partnership solutions, but these are outside the scope of this whitepaper.

4.1 Assessment Scores

The assessment scores obtained here are based on the commercial capabilities at the end of 2022. It is a fair assumption that commercial capabilities will increase significantly by the time of the SDC mission. However, it is difficult to project commercial capabilities into the 2030s, as the market is currently going through a rapid growth. It is unclear how the growth rate will change in the next ten or so years. Therefore, a conservative approach is taken by assessing the current capabilities and repeating the assessment over time before key decision points for SDC.

As it can be seen from Tables 4 and 6, the horizontal resolution capability of both commercial constellations and the L1A architecture is defined as 5 m. This is due to the fact that the SATM does not include any resolution needs beyond 5 m, and any architecture providing a resolution of 5 m or better automatically obtains the highest partial score of 1.

The Earth Science Decadal Survey (National Academies, 2019) emphasised the need for interferometric repeat pass at weekly to daily rates, resolution between 5-15 m, sensitivity to height changes between 1 and 10 mm, with a time series measurement accuracy of between 1 mm/week and 1 mm/year (depending on the duration of the time series) all the while providing continuous global monitoring of all land and coastal areas. Architectures that obtain daily global monitoring of all land and coastal areas easily exceed the cost cap due to increased in orbit duty cycles (or number of satellites) necessary. Therefore, if an SDC architecture is selected such that it provides a generally accepted solution for global monitoring, albeit at longer end of the decadal survey revisit requirements, augmentation of SDC with commercial data can reduce the revisit for areas of interest whenever necessary (e.g. geohazards).

The GOs that score higher than SDC architectures indicate potential benefits to the science community beyond routine monitoring, all of which have a higher X-band accuracy score and are regional in nature (Table 7). In other words, if areas of interest can be narrowed down using non-commercial data, these GOs may benefit from routine commercial data collections for the specific applications.

4.2 Ice-Sheet Speckle Tracking and InSAR Analyses

Ice sheets are acknowledged by the World Meteorological Organization (WMO) and the United Nations entity tasked with supporting the global response to the threat of climate change (UNFCCC) as an Essential Climate Variable (ECV) needed to make significant progress in the generation of global climate models. Several national and international programs (NASA MEaSUREs, ESA Climate Change Initiative) fund efforts to generate high quality geoinformation products for Antarctica and Greenland based on satellite remote sensing data. The SDC SATM builds on the ECV requirements.

		Accuracy		Scores	
GO	**DS Science Variable**	**L1A**	**C.C.**	**L1A**	**C.C.**
C7	Tidal flexure in the grounding zones (50 km upstream and all floating)	0.05	0.64	0.05	0.43
C9	Elevation signal of interior sub-glacial lake drainage and filling	0.05	0.64	0.05	0.18
S12	Deformation from fluid fluxes in shallow aquifers	0.29	1.0	0.29	0.43
S13	Vertical surface deformation – impact of human activities and water flow on earthquakes	0.21	0.4	0.21	0.40

Table 7. Comparative assessment of scores for the L1A architecture and commercial constellations (C.C.) for the GOs that do not follow the logarithmic trend.

Interferometric SAR data are particularly useful for ice sheet science with respect to surface velocity and grounding line measurements. Ice velocity (C1, C2, C3), and strain fields (C4, C5) are typically measured using speckle tracking (Rignot et al., 2011), where surface parallel 2D motion can be measured using a pair of acquisitions. A more accurate method is to exploit the InSAR phase; this approach requires interferograms acquired in different viewing geometries to resolve 2D motion (Mouginot et al., 2019). Figure 3 shows an example of a feature tracking result of high resolution X-band data on an Antarctic glacier. In this case data were acquired in a near-repeat track orbit, but without controlling the interferometric baseline. The high resolution data provide sufficient surface features on the glacier itself for offset tracking to work. The ultimate goal for a comprehensive data assessment is to obtain InSAR data, however, to assess the full potential of a mission, as demonstrated by the following example.

The ice-ocean interface of a glacier is a critical boundary. The grounding line delineates where ice detaches from the bed and becomes afloat and frictionless at its base. Using double difference interferometry, the flexing of the ice shelf due to differential tide levels at four acquisition times results in a dense band of fringes in the interferogram due to the vertical displacement. The upstream boundary of this fringe band is interpreted as the InSAR grounding line (related to C7 in Table 7). The approach requires the availability of 2 interferograms with the same geometry. Fast glaciers can pose a problem for missions with a longer repeat orbit due to phase decorrelation. Commercial high resolution InSAR missions with short repeat orbits do not generally satisfy the spatial coverage requirement, however, they can be used to augment agency missions like SDC with a more global coverage approach. Early results highlighting the value of a commercial InSAR data for grounding line studies are presented in (Figure 3, Ciraci et al., 2022).

4.3 Analysis of Potential Persistent Scatterers

Preliminary analysis on the interferometric potential of commercial X-band data for deformation monitoring over semi-arid land and exposed rock was also conducted through the analysis of a set of available scenes from Capella Space over the West Angelas Mine in western Australia, shown in Figure 4. The study area is a desert devoid of vegetation, which presents a good opportunity for image analysis without confounding issues of decorrelation and terrain type. Interferometric techniques can also supplement traditional change detection methods for

monitoring environmental health in and around active mines; interferometry is more sensitive to small changes on the ground and is capable of monitoring hydrological activity such as groundwater extraction through measurement of deformation as a proxy.

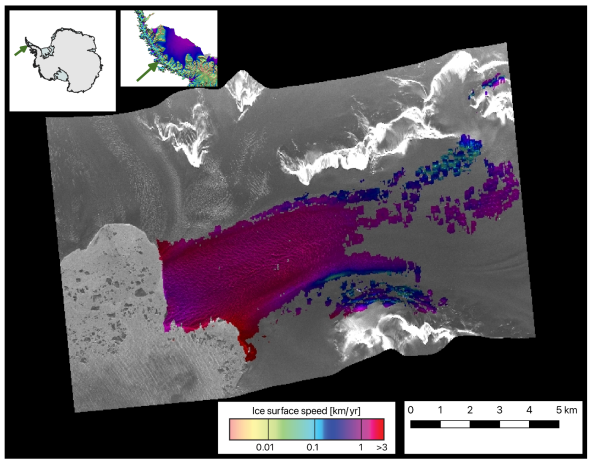

Figure 3. Feature tracking result of imagery from Capella Space over Murphy Glacier, Antarctic Peninsula.

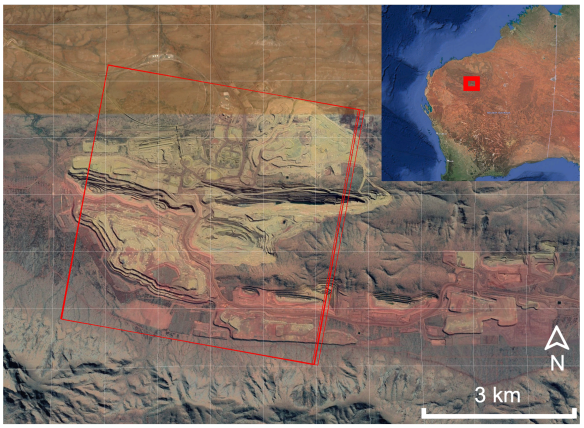

Figure 4. Coverage of imagery from Capella Space over the West Angelas Mine; area in western Australia shown in inset.

The potential performance of the scenes for use in persistent scatterer InSAR (PS-InSAR) was evaluated through the estimation of the density of potential persistent scatterer (PS) candidates. Because the scenes were described to be interferometry-feasible but were not acquired to be interferable, this preliminary analysis evaluated PS candidates not using phase-based methods but instead by using two common amplitude-based methods that are used in existing PS identification algorithms as initial filtering steps before detailed phase analysis. Results were compared with Sentinel-1B imagery that was acquired over the same area and over the same time period. Dataset parameters are shown in Table 8.

Capella imagery was corrected based on the WGS84 ellipsoid and geocoded to a 20 x 20 m grid using the GAMMA software (Wegnüller et al., 2016). Sentinel-1 imagery was processed using the 20 x 20 m Copernicus DEM for topographic correction and geocoding using a backprojection processor (Zebker, 2022). The Sentinel-1 imagery was then masked to the approximate size and area of the Capella acquisitions. Preliminary analysis of PS candidates was conducted by thresholding of calculated amplitude dispersion and signal-to-clutter ratio (SCR) of each stack, defined respectively as:

$$D_a = \frac{\sigma_a}{\mu_a} \quad (5)$$

$$\gamma = \frac{P_d}{P_c} \quad (6)$$

where σ_a is the standard deviation and μ_a the mean of the amplitude of a pixel across the image stack, and D_a is the amplitude dispersion; in (6), P_d is the power of the dominant scatterer, taken as the power of a single pixel, P_{cc} is the power of the clutter, estimated by taking the average of the immediately surrounding pixels, and γ is the SCR.

Parameter	Capella Space	Sentinel-1B
Number of scenes	6	7
Imaging mode	Spotlight	Interferometric Wide swath (IW)
Orbit pass direction	Descending	Descending
Dates	2021-07-01 to 2021-09-10	2021-07-05 to 2021-09-1
Native resolution	0.4 m x 0.5 m	5 x 20 m

Table 8. Imaging parameters for Capella Space and Sentinel-1B datasets used in the mining case study.

Figure 5 shows the comparison between the Capella and Sentinel stacks with an amplitude dispersion of 0.4 and 0.25, which are the thresholds used for initial pixel elimination during the first step of StaMPS and the original PSI algorithms, respectively (Hooper et al. 2004, Ferretti et al. 2001). Figure 6 shows the comparison between the two stacks with an SCR of 2, which is the threshold used for initial candidate selection in the STUN algorithm (Kampes, 2005), and an SCR of 10, a much more stringent threshold. The results are mixed, showing a higher estimated PS candidate density in Capella data when comparing SCR, but a higher estimated PS candidate density in Sentinel-1 data when comparing amplitude dispersion.

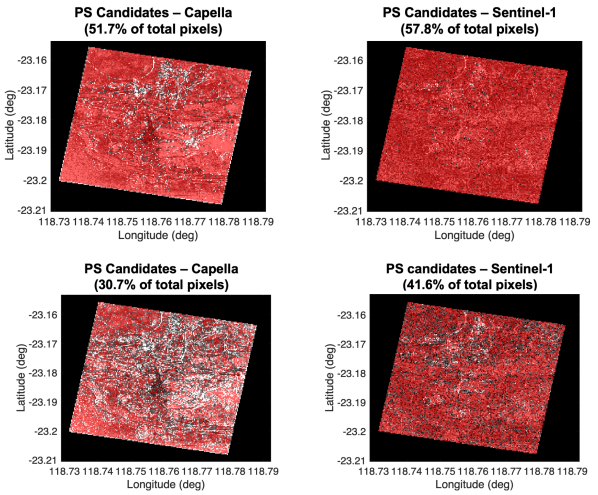

Figure 5. Comparison between Capella and Sentinel image stacks with an amplitude dispersion threshold of < 0.4 (top) and < 0.25 (bottom). The number in parentheses indicates the percentage of total pixels identified as PS candidates.

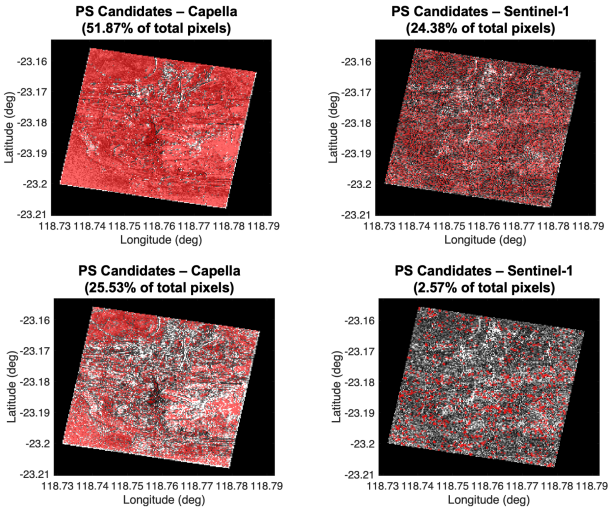

Figure 6. Comparison between Capella and Sentinel image stacks with an SCR threshold of > 2 (top) and > 10 (bottom). The number in parentheses indicates the percentage of total pixels identified as PS candidates.

The discrepancy between the two tested measures highlights the limitations of purely amplitude-based measures as effective phase proxies, given that PS candidate density is expected to scale with resolution regardless of wavelength (Huang and Zebker, 2018). The lower PS candidate density for Capella data using amplitude dispersion, in particular, is also likely due to the fact that the commercial imagery was not acquired for interferometry, resulting in an uncontrolled baseline that lowers phase stability. SCR, by contrast, is a more direct measure of relative scatterer brightness, which is higher in the higher-resolution Capella data compared to Sentinel-1 data. Capella data should show an improvement in PS candidate density detected using amplitude dispersion if acquired in orbit-controlled passes designed for interferometry. Ultimately, while this preliminary analysis indicates promise for the use of commercially acquired high-resolution SAR data in interferometric applications, future analysis with high-resolution DEMs as well as with an interferometric dataset, when available, will be required to make a further determination on the capabilities and limitations of commercially available data to augment observation of SDC GOs.

5. CONCLUSION

In conclusion, this quantitative feasibility study of the commercial sector indicates that, as is, the X-band commercial systems can have some role in meeting the observational capabilities defined in SDC's SATM. Some GOs in the SATM can benefit from commercial data either to supplement the observations of an SDC architecture or to fill a gap that is left by such an architecture. Assessing all of the SDC architectures through this framework would identify the relative benefits of commercial data for each architecture. It is important to note that, as the commercial constellation capability increases, many more GOs will benefit from this data-rich environment.

REFERENCES

Ciracì, E., Rignot, E., Milillo, P. and Dini, L., 2022, May. Evaluating Petermann Gletscher ice-shelf basal melt and ice-stream dynamics from high-resolution TanDEM-X elevation data. In *EGU General Assembly Conference Abstracts* (pp. EGU22-10979).

Ferretti, A., Prati, C., & Rocca, F., 2001: Permanent scatterers in SAR interferometry. *IEEE Transactions on geoscience and remote sensing*, 39(1), 8-20. doi.org/10.1109/36.898661

Hooper, A., Zebker, H., Segall, P., & Kampes, B., 2004: A new method for measuring deformation on volcanoes and other natural terrains using InSAR persistent scatterers. *Geophysical research letters*, 31(23). doi.org/10.1029/2004GL021737

Horst, S., Chrone, J., Deacon, S., Le, C., Maillard, A., Molthan, A., Nguyen, A., Osmanoglu, B., Oveisgharan, S., Perrine, M., Others, 2021. NASA's Surface Deformation and Change Mission Study, in: 2021 IEEE Aerospace Conference (50100).

Huang, S., & Zebker, H., 2019: Persistent scatterer density by image resolution and terrain type. *IEEE Journal of Selected Topics in Applied Earth Observations and Remote Sensing*, 12(7), 2069-2079. doi.org/10.1109/JSTARS.2019.2896038

Kampes, B., & Adam, N., 2005: The STUN algorithm for persistent scatterer interferometry. *Proceedings of FRINGE 2005*, 1-14.

Kellogg, K., Hoffman, P., Standley, S., Shaffer, S., Rosen, P., Edelstein, W., Dunn, C., Baker, C., Barela, P., Shen, Y., Guerrero, A.M., Xaypraseuth, P., Sagi, V.R., Sreekantha, C.V., Harinath, N., Kumar, R., Bhan, R., Sarma, C.V.H.S., 2020. NASA-ISRO Synthetic Aperture Radar (NISAR) Mission, in: 2020 IEEE Aerospace Conference. ieeexplore.ieee.org, pp. 1–21.

Khazendar, A., Molthan, A., Sauber, J., Bell, J., Carabajal, C., Glasscoe, M., Le Roy, A., Lucey, R., Rogers, L., Sylak-Glassman, E., Gardner, A., Jones, C., Owen, S., Reager, Rieger J.T., Siqueira, P. et al., 2021. Science and Applications Traceability Matrix [WWW Document]. Surface Deformation and Change (SDC). URL https://science.nasa.gov/science-pink/s3fs-public/atoms/files/SDC_SATM_Phase1_Final_0.pdf (accessed 1.24.23).

National Academies of Sciences, Engineering, and Medicine, Division on Engineering and Physical Sciences, Space Studies Board, Committee on the Decadal Survey for Earth Science and Applications from Space, 2019. Thriving on Our Changing Planet: A Decadal Strategy for Earth Observation from Space.

Rignot, E., Mouginot, J. and Scheuchl, B., 2011. Ice flow of the Antarctic ice sheet. *Science*, *333*(6048), pp.1427-1430.
Mouginot, J., Rignot, E. and Scheuchl, B., 2019. Continent‐wide, interferometric SAR phase, mapping of Antarctic ice velocity. *Geophysical Research Letters*, *46*(16), pp.9710-9718.

Rosen, P.A., Kumar, R., 2021. NASA-ISRO SAR (NISAR) Mission Status, in: 2021 IEEE Radar Conference (RadarConf21). pp. 1–6.

Wegnüller, U., Werner, C., Strozzi, T., Wiesmann, A., Frey, O. and Santoro, M., 2016: Sentinel-1 support in the GAMMA software. *Procedia Computer Science*, 100, 1305-1312. doi.org/10.1016/j.procs.2016.09.246

Zebker, H., 2022: Sentinel-1 Analysis Ready Data – A Convenient and Easy to Use System Producing Common-coordinate Timeseries. In *AGU Fall Meeting Abstracts 2022*, G42D-0257.

APPENDIX

In the table below, the needs are grouped for display purposes. Needs 1-8 correspond to:

1. Polarisation (Number of polarimetric channels)
2. Resolution (metres)
3. Revisit (Number of days between revisits)
4. Latency (Number of days between acquisition and data delivery)
5. Accuracy (Percent accuracy based on performance tool, literature survey or heuristic evaluation)
6. Coverage:
    - G = Global
    - C = Continental
    - R = Regional
    - L = Local
7. Large area imaging capability (Yes if needed for the GO or No)
8. InSAR capability (Yes if needed for the GO or No)

“&” is entered for GOs that have multiple methods that and not all of them require InSAR. Same thing is true for Large area imaging.

Modifiers “k” indicate “times 1000”.

GO	DS Science Variable	Parameters							
		1	**2**	**3**	**4**	**5**	**6**	**7**	**8**
C1	Mean flow of fast flowing outlet glaciers, grounded and floating (>50 m/yr)	1	5	7	90	1.00	C	&	Y
C2	Mean flow of slow flowing ice-sheet interiors (<50 m/yr)	1	500	365	90	1.00	C	Y	Y
C3	Mean flow of large mountain glaciers	1	3	60	90	1.00	R	N	Y
C4	Strain rates at shear margins (grounded ice)	1	5	30	90	1.00	R	N	Y
C5	Strain rates associated with fracture and calving and ice mélange	1	5	0.25	90	1.00	R	&	N
C6	Geometry of ice mélange	1	10	0.25	90	0.5	R	N	&
C7	Tidal flexure in the grounding zones (50 km upstream and all floating)	1	50	7	90	0.64	R	N	Y
C8	Basal friction inverted from temporal changes in velocity	1	5	0.25	90	1.00	R	Y	Y
C9	Elevation signal of interior sub-glacial lake drainage and filling	1	50	7	90	0.64	R	Y	Y
C10	Circumpolar fine scale sea ice motion & deformation	1	100	1	90	0.65	C	Y	N
C11	Sea ice ridge and lead evolution, polynya formation, brine formation, and heat flux	1	100	1	90	0.65	C	Y	N
C12	Marginal/coastal sea ice zone mechanics and fluxes	1	100	1	90	0.65	R	Y	&
C13	Sea ice formation and distribution	1	100	1	90	0.65	C	Y	N
E1	Absolute Soil Moisture	1	20	3	1	0.35	G	N	N
E2	Relative Soil Moisture	1	20	3	1	0.35	G	N	N
E3	Freeze/Thaw Boundary Dynamics (Frozen/Not Frozen)	1	20	7	7	0.35	R	N	N
E4	Vegetation Structure (canopy height & vertical distribution)	2	20	14	14	0.35	G	N	Y
E5	Above ground vegetation biomass & biomass change	2	20	14	14	0.6	G	N	N
E6	Change in land cover due to flooding, wildfire, wind, insects, anthropogenic	2	20	14	14	0.5	L	Y	N
E7	Agricultural Management (Active crop area, crop class, crop yield, crop practices)	2	20	14	14	0.5	R	Y	N
E8	Classification of rice and aquaculture	2	20	14	14	0.5	R	Y	N
E9	Measure inland and coastal wetlands areas	2	20	14	14	0.35	R	N	N
E10	Measure relative water level changes in wetlands	2	20	14	14	0.35	R	N	Y
H1	Snow Water Equivalent (SWE)	1	4k	3	7	0	G	N	Y
H2	SWE	2	4k	3	7	0	G	N	N
H3	Latent heat flux (soil moisture)	4	200 k	0.5	7	0.35	G	Y	N
H4	Recharge rates (soil moisture)	4	200 k	3	7	0.35	G	Y	N
H5	Fire prediction (fuel load)	4	200 k	3	7	0.35	G	Y	N
H6	Drought monitoring (soil moisture)	4	1k	7	7	0.35	G	Y	N
H7	Recharge rates (Groundwater subsidence)	1	100	3	1	1	C	Y	Y
H8	Inundated area	2	10	0.5	0.1	0.35	C	N	N
S1	Volcanic Systems and Hazards, Land surface deformation	1	10	1	365	0.03	L	N	Y
S2	Earthquake Cycle and Hazards, Land surface deformation	1	50	1	365	1.00	C	Y	Y
S3	Landslides Hazards, Land surface deformation	1	10	30	365	0.16	R	N	Y
S4	Rapid Deformation Map Acquisitions	1	10	7	2	0.52	L	N	Y
S5	Sea Level Rise, 3D Surface deformation vectors on ice sheets, Ice Velocity	1	100	30	365	1.00	C	Y	Y
S6	Sea Level Rise, Vertical motion of land along coastlines	1	50	6	365	0.31	C	Y	Y
S7	Landscape Change – Quantify G decadal landscape change, Land Surface, Soil Moisture Deformation	1	10	7	365	0.5	G	Y	Y

GO	DS Science Variable	Parameters							
		1	**2**	**3**	**4**	**5**	**6**	**7**	**8**
S8	Landscape Change – Content of Near Surface Materials, Reflectance for freeze/thaw, Reflectance for snow depth/snow water equivalent	1	100	7	365	1	G	Y	N
S9	Energy Change – Effect of Convection, Plate motion and deformation	1	100	30	365	0.41	C	Y	Y
S10	Groundwater Flow and its impact on geological processes and water supply, Land surface deformation	1	10	7	365	1	C	Y	Y
S11	Measure Fluxes in and out of groundwater system	1	10	6	365	0.60	C	Y	Y
S12	Deformation from fluid fluxes in shallow aquifers	1	5	7	365	1	R	N	Y
S13	Vertical surface deformation – impact of human activities and water flow on earthquakes	1	5	7	365	0.4	R	N	Y
S14	Discovery & Management – Map energy, mineral, agricultural and natural resources for improved management	1	30	7	365	0.24	G	Y	N
W1	Energy balance (soil moisture)	4	1k	0.5	7	0.35	G	Y	N
W2	Weather prediction (soil moisture)	4	1k	0.5	1	0.35	G	Y	N
G1	Geohazards: Volcanic Systems and Hazards, Land surface deformation	1	10	7	0.1	0.03	L	N	Y
G2	Geohazards: Earthquake Cycle and Hazards, Land surface deformation	1	10	1	0.1	1.00	L	N	Y
G3	Geohazards: Landslides Hazards, Land surface deformation	1	10	30	0.5	0.16	L	N	Y
G4	Geohazards: Rapid Deformation Map Acquisitions	1	10	1	0.1	1.00	L	N	Y